Macromolecular Research, Vol. 19, No. 9, pp 883-890 (2011)
DOI 10.1007/s13233-011-0901-1
www.springer.com/13233

High Electrically Conductive Polyaniline/Partially Phosphorylated Poly(vinyl alcohol) Composite Films *via* Aqueous Dispersions

Fei Chen and Peng Liu*

State Key Laboratory of Applied Organic Chemistry and Institute of Polymer Science and Engineering, College of Chemistry and Chemical Engineering, Lanzhou University, Lanzhou 730000, China

Received November 29, 2010; Revised February 27, 2011; Accepted April 1, 2011

Abstract: A novel low-cost approach was developed for the preparation of high electrically conducting composite films with high comprehensive properties. The polyaniline (PAn)/partially phosphorylated poly(vinyl alcohol) (P-PVA) dispersions were synthesized by the chemical oxidative polymerization of aniline in aqueous acidic (1 M HCl) media containing the partially phosphorylated poly(vinyl alcohol) (P-PVA), which can be cast directly to form smooth and mechanically robust composite films. The electrical, thermal, and mechanical properties of the PAn/P-PVA composite films were affected by the feeding ratio of aniline in polymerization. The uniform composite films showed a higher degree of crystalline orientation and higher electrical conductivity than those of the PAn/PVA films prepared with the same feeding ratio of aniline.

Keywords: conductive polymer, composite films, casting, mechanical properties.

Introduction

Polyaniline (PAn), a well-known intrinsic conducting polymer (ICP), shows the unique features such as excellent electrical conductivity, good environmental stability, chemical redox reversibility and ease of synthesis.[1-4] It exhibits a great potential in many fields, such as sensors,[5] switchable membrane,[6] organic storage batteries,[7] electrochromic displays,[8] static electricity dissipation,[9] electromagnetic shielding devices,[10] anticorrosion coatings,[11] and so on. However, some potential applications have not yet to be exploited because of its poor processability. To improve its processability, various approaches have been developed, such as introducing side groups to PAn chains,[12,13] preparing PAn dispersion with a soluble polymeric stabilizer,[14,15] synthesizing PAn/thermoplastic composites in the presence of a thermoplastic polymer,[16,17] and blending PAn with soluble polymer.[18,19]

Among the above approaches, preparing colloidal PAn dispersion by dispersion polymerization in the presence of a soluble polymeric stabilizer is a widely accepted one. In this way, conducting composites are synthesized from the respective monomer in the presence of a solution of a preformed polymer so that the macroscopic precipitation of the former can be prevented.[20] Poly(vinyl alcohol) (PVA) has been extensively used as the polymer matrix in view of its non-toxic, water-soluble, good film-forming capacity and possible coupling of charge transport with the motion of its hydroxyl groups.[20,21] In addition, PVA was proved to be used as the polymeric stabilizer of polyaniline dispersions.[20,22] The mechanism of polymerization,[23,24] morphology[25] and electrical conductivity of PAn/PVA particles,[23,26] and thermal and mechanical properties[23,27] and ion exchange properties[28] of PAn/PVA composite films had been widely reported in recent years.

However, the water resistance, mechanical properties, and even the electrical property of the PAn/PVA composite films were found far from satisfactory. These drawbacks still limit the application of PAn/PVA composite films. The use of acidic phosphate ester (APES) started with the idea of 'doping-induced processability', in which the soluble groups can be introduced to PAn as an inherent part of the dopants.[29] Partially phosphorylated poly(vinyl alcohol) (P-PVA) is a phosphoric ester prepared by the phosphorylation of PVA with phosphoric acid.[30] P-PVA exhibits higher water resistance and mechanical property than PVA[31] and can be used as metal complexes, ionic conducting polymer materials,[31] and anionic polyelectrolyte hydrogel.[32]

In the present work, the PAn/P-PVA composite films with high comprehensive performance were developed innovatively. In this system, P-PVA was used simultaneously as the co-dopant, the stabilizer, and the polymer matrix. Firstly, the colloidal PAn/P-PVA dispersions with good dispersion stability were synthesized by the chemical oxidative polymerization of aniline in 10 wt% P-PVA aqueous solution. Then, the PAn/P-PVA composite films were obtained by the

*Corresponding Author. E-mail: pliu@lzu.edu.cn

casting of the colloidal PAn/P-PVA dispersions. The electrical and physical properties of the composite films have been investigated in comparison with the PAn/PVA composite films prepared under the similar conditions.

Experimental

Materials. Poly(vinyl alcohol) (PVA: P_n=1788±50, M_w= 76, 500-80, 800) with a degree of hydrolysis of 88% was obtained from Tianjin Chemical Reagents Company. Phosphoric acid (H_3PO_4, 85%), urea ($(NH)_2CO$, 99.9%), aniline (99.9%), ammonium peroxydisulftate (APS, 99.9%), hydrochloric acid (HCl, 36~38%), and other reagents used were all analytical grade, supplied by Baiyin Chemical Agents Company, China.

Partially Phosphorylated Poly(vinyl alcohol). Partially phosphorylated poly(vinyl alcohol) (P-PVA) was prepared by the phosphorylation of PVA with phosphoric acid in an aqueous media (Scheme I).[29,33] Firstly, 94.0 g phosphoric acid, 20.0 g PVA and 2.4 g urea were added to 100 mL of distilled water in a flask and stirred for 8 h at 50 °C. The mixture was heated to 95 °C and stirred thoroughly for about 6 h, and a yellowish-white colloidal solution was obtained. The resulting solution was precipitated from ethanol to obtain the white precipitate P-PVA. Finally, the white precipitate was dried in vacuum at 50 °C. In this paper, the degree of substitution (DS) of the P-PVA was 12.9 mol%, determined by pH titration and molybdenum blue method.[31]

Colloidal PAn/P-PVA Dispersions. The colloidal PAn/P-PVA dispersions were synthesized by the polymerization of aniline in aqueous acidic (1 M HCl) media containing P-PVA as follows: 10 g P-PVA was introduced into a 250 mL round-bottom flask containing 100 mL distilled water, and the temperature of the system was raised to 80 °C to dissolve the P-PVA. Then the aqueous P-PVA solution was cooled to room temperature and charged with a certain amount of HCl to form an aqueous acidic (1 M HCl) solution of P-PVA. Certain amount of aniline was added into the P-PVA solution under continuous stirring. The system was cooled at 5 °C followed by the addition of 50 mL 1.0 M HCl solution of APS with the mole ratio of aniline to APS of 2:1. The polymerization was carried out for 8 h at about 5 °C and the dark-green PAn/P-PVA colloidal dispersion (with the volume of 150 mL) was obtained in each experiment (Table I).

After the resulting dark-green PAn/P-PVA colloidal dispersion was dialyzed against distilled water for 24 h to ensure the complete removal of the un-reacted monomer and oxidant, a series of the purified dark-green colloidal dispersions with different feeding ratios (based on the compositions of aniline and P-PVA in the polymerization) of aniline ranging from 4.89 to 38 wt% were obtained.

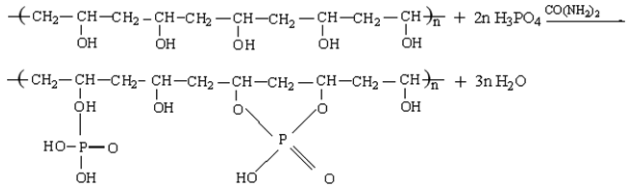

Scheme I. Synthesis route to P-PVA.

Table I. Synthesis of PAn/P-PVA Nanoparticles in 1 M Aqueous HCl Solution

Samples	Aniline (mL)	P-PVA (g)	APS (g)	Feeding Ratio of Aniline (wt%)
S-1	0.5	10	0.626	4.89
S-2	1.0	10	1.253	9.27
S-3	2.0	10	2.503	16.96
S-4	3.0	10	3.755	23.46
S-5	4.0	10	5.007	29.00
S-6	5.0	10	6.259	33.81
S-7	6.0	10	7.510	38.00

PAn/P-PVA Composite Films. For preparation of the composite films, measured amounts of the purified PAn/PVA colloidal dispersions were cast on glass sheets, dried in air at room temperature, prior to being stripped off from the sheets. And then, the films were re-doped by being immerged in 1 M HCl solution for 24 h. Finally, the films were dried again at 40 °C. For comparison, the PAn/PVA colloidal dispersions and the PAn/PVA composite films were also prepared according to the similar method as the PAn/P-PVA.

Characterizations. The FTIR measurements (Impact 400, Nicolet, Waltham, MA) were carried out with the KBr pellet method. X-ray diffraction (XRD) analysis of the composite films was performed using a 3 kW Rigaku D/MAX 2000 diffractometer equipped with the CuKα radiation in the reflection mode. Thermogravimetric analysis (TGA) results were obtained with a TA Instrument 2050 thermogravimetric analyzer at a heating rate of 10 °C/min from 25 to 800 °C under a nitrogen atmosphere. Differential scanning calorimetry (DSC) analysis of the composite films was carried out in the temperature range 30-300 °C in a Mettler TA4000 system thermal analyzer with a heating rate of 10 °C/min under nitrogen atmosphere.

The morphology and particle size of the PAn/P-PVA particles were characterized with a JEOL JEM-1200EX/S transmission electron microscope (TEM) using the water-diluted colloidal PAn/P-PVA dispersion samples. The scanning electron microscopy (SEM) micrographs of the gold coated composite films were taken with a JEOL JSM-6701F Scanning Electron Microscope operated at 25 kV.

The electrical conductivity of the composite films was measured by the four probe linear contact technique using an ADVANTEST R6142 Programmable DC Voltage/Current Generator and a Solartron S17071 precision digital Voltmeter as the current source.

Measurements. In order to measure the moisture regain capacity of the films, all film samples were dehydrated and exposed to a desiccator maintaining 70% relative humidity inside until a constant weight was reached. From the weight regain, the moisture absorption (wt%) was calculated.

The water-resistance property was determined by the following procedure: the dried films were immersed into distilled water at 25 °C, the appearance of the films was observed at regular interval. And the water-resistance property can be indicated by the time that the films could remain surface intact.

The mechanical properties were determined by measuring the tensile strength of the film at breakage on an Instron (Model 1000) mechanical test machine. The films were cut into the standard shape and the values plotted are averages for three samples.

Results and Discussion

PAn/P-PVA Nanoparticles. The TEM images of the PAn/P-PVA nanoparticles prepared with different feeding ratios of aniline in the polymerization are shown in Figure 1. The spherical particles were obtained when the feeding ratios of aniline ranged from 4.89% (S-1) to 16.96% (S-3); the rice-like particles were produced when the feeding ratios of aniline were 23.46% (S-4) and 29.00% (S-5); and the coral-like particles were formed when the feeding ratios of aniline were 33.81% (S-6) and 38.00% (S-7). In addition, the diameters of the PAn/P-PVA nanoparticles increased gradually with an increasing in the feeding ratio of aniline. The diversity of particles shape is a common phenomenon in the synthesis of PAn. The shape of particles such as sphere, rice, needle, or coral is determined by the balance between the adsorption rate of stabilizers and the formation rate of the primary PAn particles.[22] A relatively adequate amount of P-PVA will led to the formation of the spherical particles with smaller particle size. In addition, the colloidal PAn/P-VA dispersions were very stable when the feeding ratios of aniline were lower than 33.81%. No precipitation was observed in these dispersions even after eight months, and the particle size distributions were almost unchanged for one year because of the stabilizing of the P-PVA.[34]

The FTIR spectra of the P-PVA, the PAn emeraldine salt form (PAn-ES), and the PAn/P-PVA samples are shown in Figure 2. In the spectrum of P-PVA, the characteristic bands of the O-H stretching around 3250 cm^{-1}, the -CH_2 stretching (symmetric and asymmetric) at 2903 and 2810 cm^{-1}, the C-H bending at 1407 cm^{-1} are observed, and the absorbance peak at 1026 cm^{-1} is attributed to the stretching frequency of the -P-O-C- groups, and the strong absorbance peak at 1690 cm^{-1} is assigned to the stretching vibration of the -P=O- groups.[35] In the spectrum of the PAn ES, the characteristic peaks at 1502 and 1630 cm^{-1} are assigned to the non-symmetric benzene ring stretching vibration, the bonds around

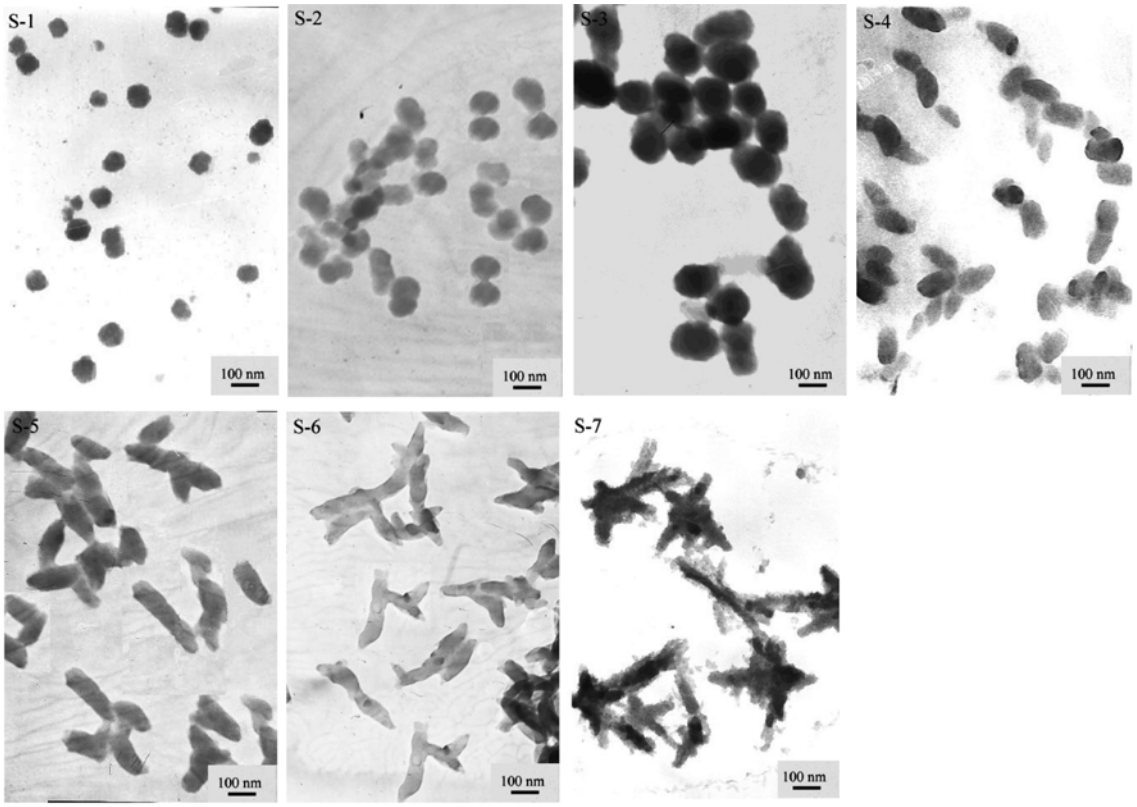

Figure 1. TEM images of the PAn/P-PVA nanoparticles.

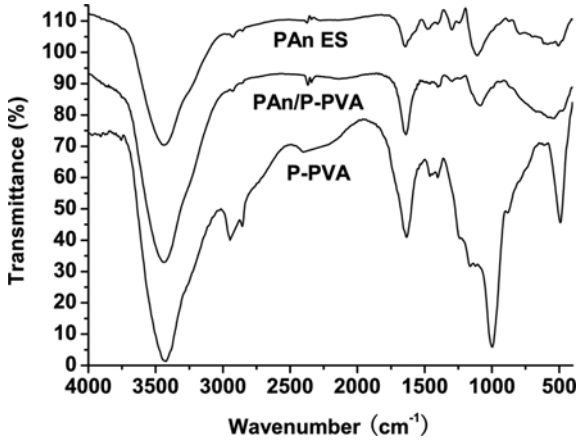

Figure 2. FTIR spectra of the P-PVA, the PAn ES, and the PAn/P-PVA samples.

1280 cm^{-1} are attributed to the stretching vibration of the C-N (mode of -N-benzenoid-N-),[36] the peak at 1130 cm^{-1} is assigned to the in-plane-bending vibration of the C-H (mode of -N=quinoid=N- and quinoid=N^{+}H-benzenoid),[37] and the peak at 3525 cm^{-1} is assigned to the N-H stretching, respectively. In the spectrum of the PAn/P-PVA nanoparticles, the strong absorbance peak at 1060 cm^{-1} is assigned to the overlap of the absorbance frequency of the -P-O-C- groups of P-PVA and the in-plane-bending vibration of the C-H of PAn. The absorbance peak at 1441 cm^{-1} is assigned to the C-O bonds, and the absorbance peak at 1690 cm^{-1} is assigned to the -P=O- groups of P-PVA. The obvious increasing of the absorbance intensity around 3390 cm^{-1} of the PAn/P-PVA samples is related to the -OH stretching, compared with that of the PAn ES. The result suggests that the P-PVA molecules had been adsorbed and/or doped in the PAn nanoparticles.

TGA analysis was used to measure the thermal properties of the PAn/P-PVA nanoparticles (Figure 3). The P-PVA undergoes three main degradation steps: the slight weight decrease of the P-PVA below 100 °C is due to the moisture-losing, and the mass loss take place up to 280 °C is regarded as the H-boned water, whereas the large decrease after 280 °C is attributed to the breakage of the main chain.[21] PAn ES also exhibits three degradation steps: the initial weight loss of about 8.0% up to 100 °C is attributed to the remainder of water and un-doped HCl, the weight loss about 5% in the temperature range of 100-300 °C is due to the de-doping of HCl, and the mass loss after 250 °C probably due to the thermal degradation of PAn.[27] TGA cures of the PAn/P-PVA nanoparticles roughly combined the profile of the P-PVA and PAn. Two main weight losing stages are found: the mass loss occurred in the temperature range of 200-300 °C is the superposition of the controlled release of the H-boned water of the P-PVA and the de-doping of HCl doped, and the sharp mass region at above 480 °C is mainly due to the breakage of the main chains of both polymers (P-PVA and PAn). It can be found that the thermal stability of the P-PVA had been improved obviously in the present of PAn and the doping structure with the ester of P-PVA as co-dopant is more stable than the PAn ES (doped with HCl). The PAn/P-PVA nanoparticles could not be de-doped and expected to be conducting up to 200 °C.

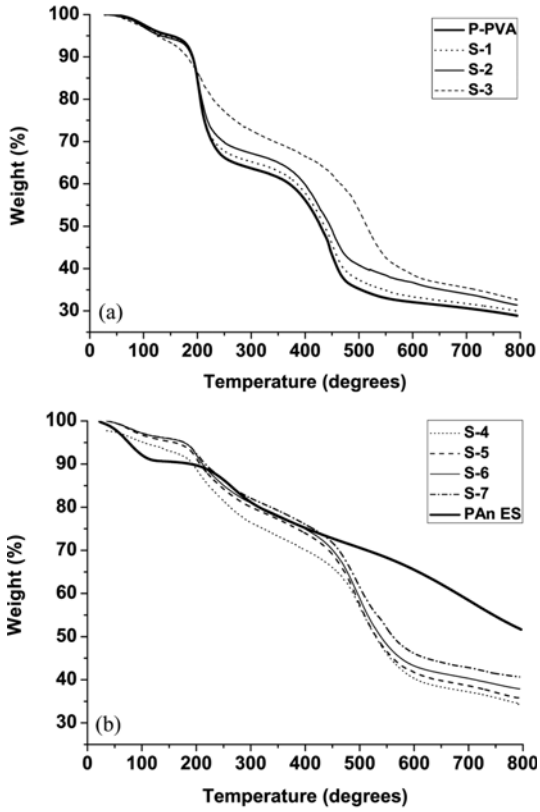

Figure 3. TGA curves of the P-PVA, the PAn ES, and the PAn/P-PVA samples.

Composite Films. The SEM micrographs of the films of pure P-PVA and the composite films of the PAn/P-PVA samples are shown in Figure 4. For the pure P-PVA film, phosphorylated polymer chains interconnected each other which led to a unique network-like morphology. Once PAn was introduced into the P-PVA matrices, the original structure of the P-PVA was disappeared in the PAn/P-PVA composite film (S-1). Increasing the feeding ratio of aniline, the rectangular single crystals of the P-PVA with high degree of crystalline orientation could be observed from the PAn/P-PVA composite films (S-2, S-3, and S-4). Upon further increasing the feeding ratio of aniline, a larger amount of crystals (including rectangular single crystals) could be found in the PAn/P-PVA composite films (S-5, S-6, and S-7).The existence of the large amount of the crystals might indicate that P-PVA acted as a polar co-dopant and interacted strongly with PAn particles in the aqueous system of the dispersion polymerization.[38]

XRD patterns of the PVA, P-PVA, PAn/PVA, and PAn/P-PVA films (S-3) are shown in Figure 5 (Figure 5(a): PVA

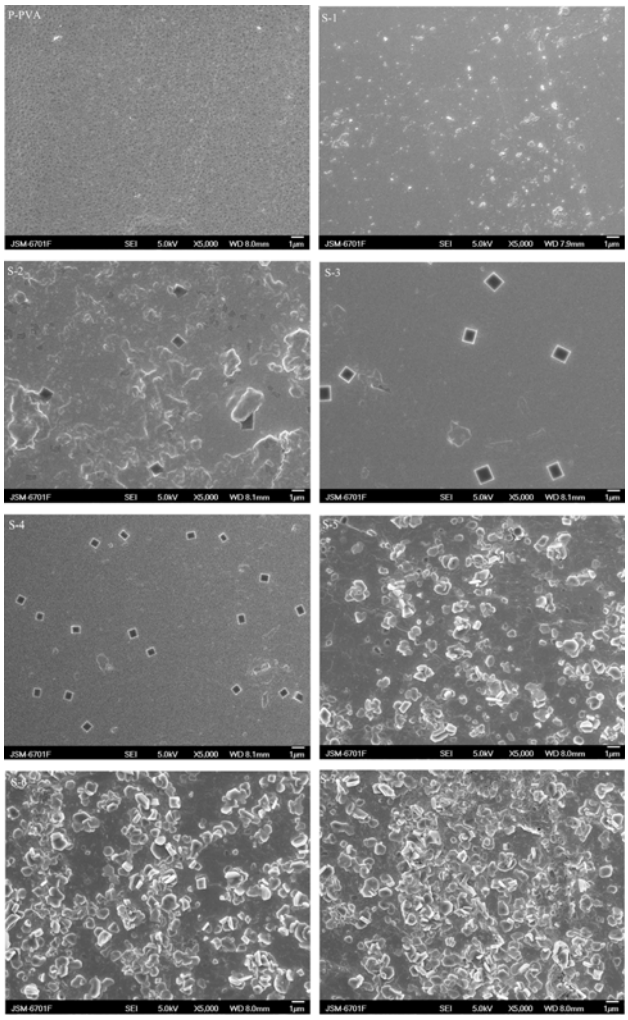

Figure 4. SEM photographs of the P-PVA film and the PAn/P-PVA composite films.

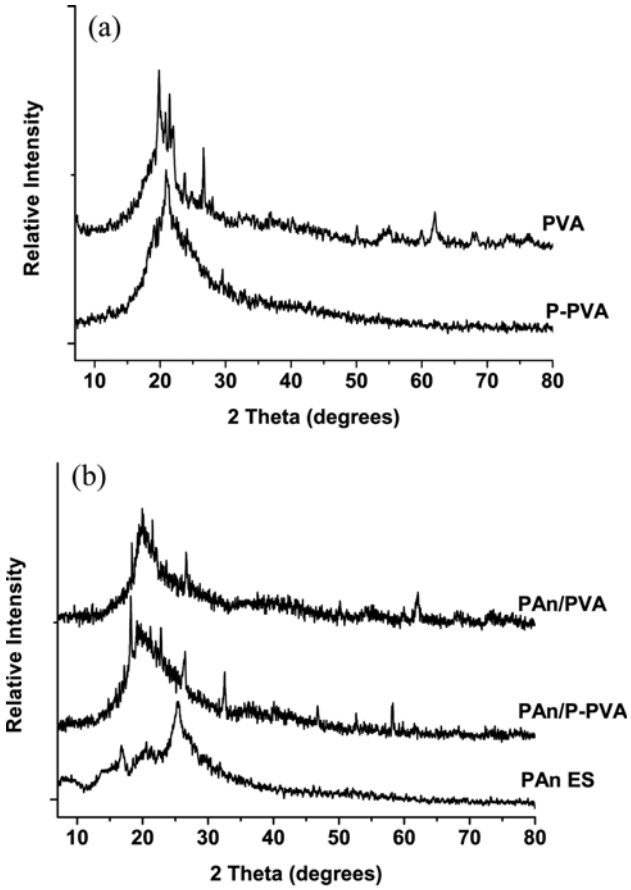

Figure 5. XRD patterns of the films: (a) PVA, P-PVA and (b) PAn ES, PAn/PVA, and PAn/P-PVA(S-3).

and P-PVA; Figure 5(b): PAn/PVA, PAn/P-PVA, and PAn ES). For the pure PVA films, there two sharp peaks at 2θ= 20.2° and 20.9°, which indicate a crystalline structure. Comparing with the pure PVA films, the crystalline peaks at around 2θ=20° of the P-PVA films broaden and the intensity was weaker due to the introduction of phosphorylate ester groups, as reported previously.[31] Meanwhile, the crystalline peaks of the PAn ES appeared at 2θ=6.7°, 20.5°, 25.4°, 26.4° and 29.4° were attributed to the periodicity perpendicular to the polyaniline chain in its emeraldine salt form (PAn ES),[39] indicating that PAn ES was partly crystalline therein. For the PAn/PVA and PAn/P-PVA composite films (both with the feeding ratio of aniline of 16.96 wt%), the numerous peaks at around 2θ=20° due to PVA crystalline, the small sharp peak at about 2θ=18.2° also was resulted from the crystalline phase with the polymeric matrix. For the PAn/P-PVA composite films, the novel and clear peak at 2θ=32.6° may be due to the rectangular crystals of the P-PVA matrix.[40] Comparing with the PAn/PVA composite films, the intensity ratio of the small diffraction peak at about 2θ=26.4° (related to the PAn ES) of the PAn/P-PVA composite films was higher, indicating that the more homogeneous protonation of PAn achieved by the polymerization in the present of phosphorylate ester groups.[38] And the crystallization of the phosphorylate ester side groups with high degree of orientation and the more homogeneous protonation of PAn achieved by the polymerization route would be directly related to the higher electrical conductivity of the PAn/P-PVA composite films.

Figure 6 represents the DSC thermograms of the pure P-PVA film, PAn ES power and two the PAn/P-PVA composite films. It can be seen that the melting endotherm (T_m) of P-PVA is around 196 °C. On the other hand, PAn ES showed a broad endotherm corresponding to the release of HCl and moisture within 80-100 °C followed by a weak endotherm around 250 °C relating to the morphological changes at elevated temperatures.[40] Features of the PAn/P-PVA films combined the characteristics of the PAn ES with P-PVA, indicating that the composites successfully combined the physical properties of both the components.

The electrical conductivity of the PAn/P-PVA composite films was measured and the results are shown in Figure 7.

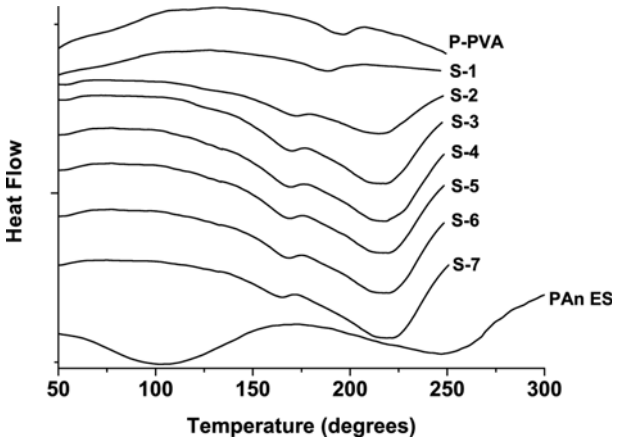

Figure 6. DSC curves of the P-PVA film, the PAn/P-PVA composite films, and the PAn ES power.

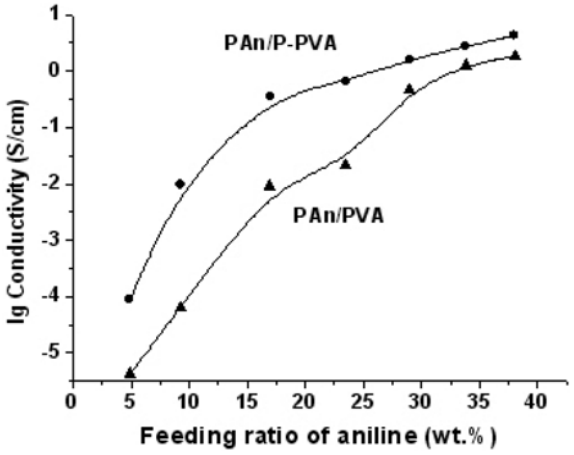

Figure 7. Effect of the feeding ratio of aniline on the electrical conductivity of the PAn/P-PVA and PAn/PVA composite films.

By varying the feeding ratio of aniline from 4.89 to 38 wt%, the electrical conductivity of the PAn/P-PVA composite films increased in the range of 8.8×10^{-5}-4.29 S/cm. A similar trend was observed from the PAn/PVA composite films. It also can be observed that the PAn/P-PVA composite films behaved like a classical percolating one (an increase of conductivity by100-fold at a feeding ratio of aniline of 4.86 wt%) while the percolation threshold value of the PAn/PVA composite films was 9.27 wt%. The percolation threshold value of the PAn/PVA composite films is consistent with these values in earlier reports describing the dispersion polymerization of aniline in presence of different water soluble and insoluble polymers.[41,42] When PVA were used as matrix, the percolation threshold values generally ranged from 7 to 10 wt%. The PAn/P-PVA composite films showed the comparatively higher conductivity and lower percolation threshold value than the PAn/PVA composite films due to the higher dope level achieved by HCl and P-PVA which played the role of co-dopant in this system[34] and the more ordered structure of crystalline which could drive exclusion

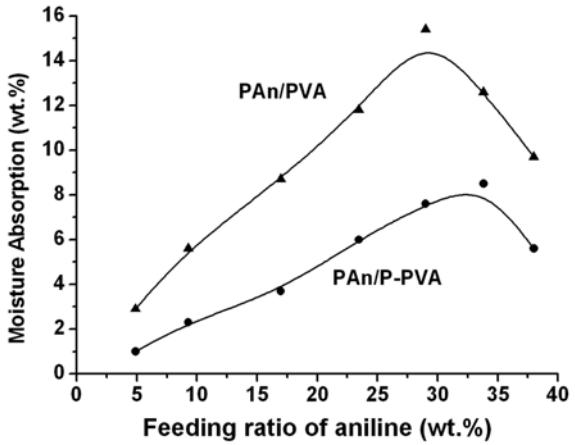

Figure 8. Effect of the feeding ratio of aniline on the moisture absorption of the PAn/P-PVA and PAn/PVA composite films.

of the conducting polymer into the interspherultic region.

Moisture absorption results of the composite films are compared in Figure 8. It is found that the moisture absorption value of the pure P-PVA film was lower than that of the pure PVA film because of the phosphorylation and the partially crossilinking during the phosphorylation with phosphoric acid. Meanwhile, the moisture absorption of the PAn/P-PVA composite films was generally lower than those of the PAn/PVA composite films prepared with the same feeding ratio of aniline. It also can be observed that the moisture content of the PAn/P-PVA composite films increased with increasing the feeding ratio of aniline up to 33.81 wt%, then it decreased. A similar trend was observed from the PAn/PVA composite films. When the feeding ratio of aniline was low, the PAn particles were embedded within the core of the P-PVA network, the moisture absorption value was much lower. On increasing the feeding ratio of aniline, the resultant excrescent PAn particles separated from the P-PVA matrix and absorbed moisture, and the moisture absorption increased substantially.

The dried films were immersed into distilled water at 25 °C, and the appearance of the films observed at regular interval. The PAn/P-PVA composite film (S-3) and the PAn/PVA composite film were prepared with the same feeding ratio of aniline of 16.96 wt%. Figure 9 shows the appearance of the two films after being immerged into distilled water at regular interval: 0 (Figure 9(a)), 1 (Figure 9(b)), 3 (Figure 9(c)), and 10 days (Figure 9(d)). It can be seen from Figure 9(a) that the smooth, flexible, mechanically robust films could be prepared from both of the PAn/P-PVA dispersion and the PAn/PVA dispersion by the casting method. There was no change occurred on the surface of both the two composite in 1 day. After 3 days, some bubbling and pitting were observed in the PAn/PVA composite film whereas the PAn/P-PVA composite film remained the intact surface. After 10 days, the PAn/PVA film showed signifi-

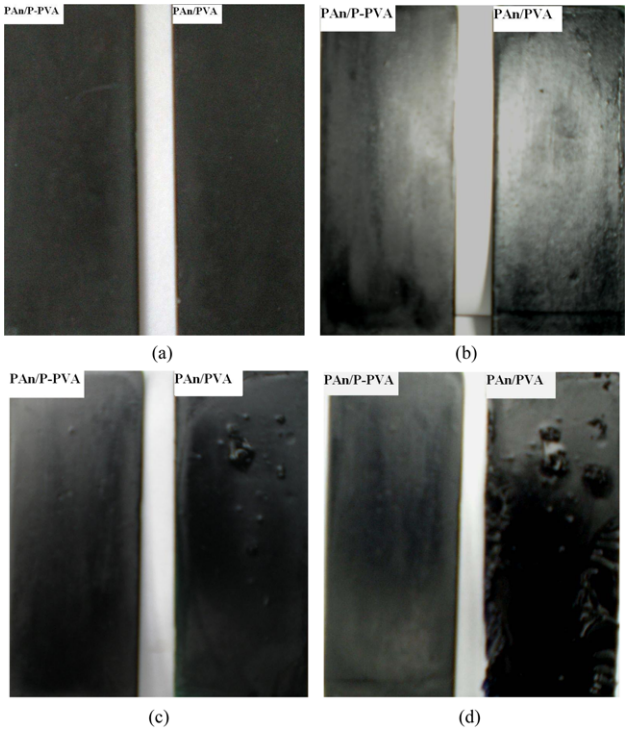

Figure 9. Photographs of the PAn/P-PVA (S-3) and PAn/PVA composite films after being immerged in water for (a) 0, (b) 1, (c) 3, and (d) 10 days.

cantly swelling accompanied by bubbling and pitting while the PAn/P-PVA film was still intact. By varying feeding ratio of aniline from 4.89 to 38 wt%, the water-resistance property of the PAn/P-PVA films was generally higher than the corresponding PAn/PVA films. It indicated that the water-resistance property of the PAn/P-PVA composite film was higher than that of the PAn/PVA film due to the good water-resistance property of the P-PVA matrix and the intensive interaction between the PAn particles and the P-PVA matrices.

The mechanical properties of the pure P-PVA and the composite films with various feeding ratio of aniline were determined. The results including the Young's modulus, the tensile strength and the elongation at break are shown in Table II. P-PVA itself can form good quality films with appreciable Young's modulus and tensile strength. Once PAn was introduced into P-PVA, the tensile strength of the composite films suffered a remarkable reduction. However, the tensile strength increased in some extent with an increasing in the feeding ratio of aniline, similar as the trend of the PAn/PVA composite films.[23] As its role in the PAn/PVA composite films, small amounts of PAn must disturb the P-PVA network resulting in a lower value for the tensile strength. Increasing the feeding ratio of aniline, a more uniform combination of PAn/P-PVA would result an increase of the tensile strength. Upon further increasing the feeding ratio of aniline, the tensile strength decreases again. Owing to higher feeding ratio of aniline, some free PAn particles might separate from the P-PVA matrices and gather on the surface of the film, causing irregularity within the sample which may cause such lowering effect.[43] On the other hand, the value of elongation at break was improved dramatically upon the introducing PAn into P-PVA. When the feeding ratio of aniline increased to 16.96 wt%, the PAn/P-PVA composite films could be stretched up to 198.4%. This value is also higher than the value (of 185%) of the PAn/PVA composite films.[23] With increasing the feeding ratio of aniline, the Young's modulus of the samples was enhanced in the earlier stage and weakened later; there was a maximum of Young's modulus (2.45 MP) at an feeding ratio of aniline of 16.96 wt%. In addition, the Young's modulus of the PAn/P-PVA composite film was clearly improved, compared with the PAn/PVA composite films reported previously.[23] The tensile strength is comparable with mechanical properties of the PAn/PVA composite films prepared under the similar experimental condition and similar trends are observed (Figure 10). Each of the tensile strength of the PAn/P-PVA composite film is higher in some extent than

Table II. Mechanical Properties of the PAn/P-PVA Composite Films

Samples	Young's Modulus (MPa)	Tensile Strength (MPa)	Elongation at Break (%)
P-PVA	2.08	39.43	110.25
S-1	2.23	30.20	166.33
S-2	2.30	32.07	175.80
S-3	2.45	35.38	198.40
S-4	2.14	28.25	164.33
S-5	1.94	24.84	175.00
S-6	1.73	16.85	150.65
S-7	1.56	14.99	145.24

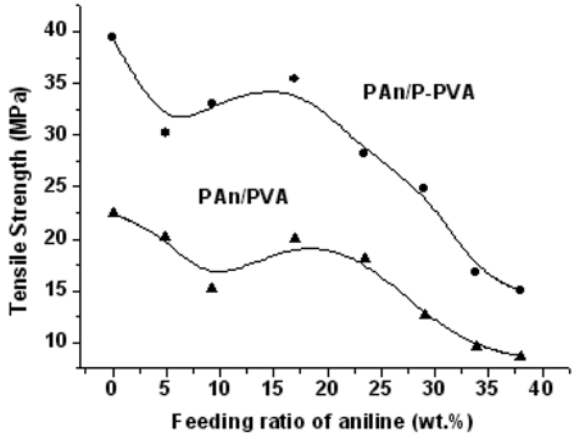

Figure 10. Effect of the feeding ratio of aniline on the tensile strength of the PAn/P-PVA and PAn/PVA composite films.

the corresponding PAn/PVA film due to the phosphate side groups which could improve the interfacial property of the composites and the crystallizablility of the polymeric matrix.[41]

Conclusions

A series of the PAn/P-PVA dispersions with different feeding ratio of aniline were prepared by polymerization of aniline in aqueous acidic (1 M HCl) media containing P-PVA. It was found that the morphology of the PAn/P-PVA nanoparticles, the electrical conductivity, water-resistance property, and mechanical properties of the PAn/P-PVA composite films were affected obviously by the feeding ratio of aniline. When the feeding ratio of aniline ranged from 16.96% to 23.46%, the PAn/P-PVA nanoparticles took spherical shape, and the PAn/P-PVA composite films exhibited high degree of crystalline orientation, excellent electrical conductivity, water-resistance property, and mechanical properties.

References

(1) S. Bhadra, D. Khastgir, N. K. Singha, and J. H. Lee, *Prog. Polym. Sci.*, **34**, 783 (2009).
(2) N. Gospodinova and L. Terlemezyan, *Prog. Polym. Sci.*, **23**, 1443 (1998).
(3) S. Bhadra, N. K. Singha, and D. Khastgir, *Synth. Met.*, **156**, 1148 (2006).
(4) A. G. MacDiarmid, *Synth. Met.*, **125**, 11 (2002).
(5) M. Gururaj, N. Valery, A. Alexander, Y. Kateryna, H. Erika, and J. Margaret, *Polymer*, **51**, 2000 (2010).
(6) D. R. Franco, G. Evandro, Z. F. Jane, A. S. Marco, and A. Carlos, *J. Membr. Sci.*, **234**, 139 (2004).
(7) M. Deka, A. K. Nath, and A. Kumar, *J. Membr. Sci.*, **327**, 188 (2009).
(8) L. Zhao, Y. X. Xu, T. F. Qiu, L. J. Zhi, and G. Q. Shi, *Electrochim. Acta*, **55**, 491 (2009).
(9) R. Alan and R. John, *Macromolecules*, **33**, 5221 (2000).
(10) D. D. Lchung, *Carbon*, **39**, 279 (2001).
(11) K. Kamaraj, S. Sathiyanarayanan, S. Muthukrishnan, and G. Venkatachari, *Prog. Org. Coat.*, **64**, 460 (2009).
(12) H. K. Lin and S. A. Chen, *Macromolecules*, **33**, 8117 (2000).
(13) X. G. Li, M. R. Huang, W. Feng, M. F. Zhu, and Y. M. Chen, *Polymer*, **45**, 101 (2004).
(14) S. Tetyana, S. Jaroslav, K. Ivo, and P. Jan, *Eur. Polym. J.*, **37**, 219 (2001).
(15) B. Jia, T. Hino, and N. Kuramoto, *React. Funct. Polym.*, **67**, 836 (2007).
(16) M. V. B. Krishna, D. Karunasagar, and S. V. Rao, *Talanta*, **68**, 329 (2005).
(17) H. Chen, J. Y. Chen, K. Aoki, and T. Nishiumi, *Electrochim. Acta*, **53**, 7100 (2008).
(18) P. Nicoleta, G. Ion, I. Smaranda, and I. Gheorghe, *Synth. Met.*, **159**, 501 (2009).
(19) Y. H. Geng, Z. C. Sun, J. Li, X. B. Jing, X. H. Wang, and F. S. Wang, *Polymer*, **40**, 5723 (1999).
(20) E. G. Chatzi and C. Kiparssides, *AIChE J.*, **41**, 1640 (1995).
(21) C. Bartholome, P. Miaudet, A. Derre, M. Maugey, O. Roubeau, C. Zakri, and P. Poulin, *Compos. Sci. Technol.*, **68**, 2568 (2008).
(22) M. Mumtaz, C. Labrugere, E. Cloutet, and H. Cramail, *Langmuir*, **25**, 13569 (2009).
(23) A. Mirmohseni and G. G. Wallace, *Polymer*, **44**, 3523 (2003).
(24) N. Gospodinova, L. Terlemezyan, P. Mokreva, and K. Kossev, *Polymer*, **34**, 2434 (1993).
(25) N. Gospodinova, P. Mokreva, T. Tsanov, and L. Terlemezyan, *Polymer*, **38**, 743 (1997).
(26) P. Dutta, S. Biswas, M. Ghosh, S. K. De, and S. Chatterjee, *Synth. Met.*, **122**, 455 (2001).
(27) Z. Zhang and M. Wan, *Synth. Met.*, **128**, 83 (2002).
(28) T. Nagaoka, H. Nakao, T. Suyama, K. Ogura, M. Oyama, and S. Okazaki, *Anal. Chem.*, **69**, 1030 (1997).
(29) Q. G. Wang, X. H. Wang, J. Li, X. J. Zhao, and F. S. Wang, *Synth. Met.*, **148**, 127 (2005).
(30) J. W. Rhim, H. B. Park, C. S. Lee, J. H. Jun, D. S. Kim, and Y. M. Lee, *J. Membr. Sci.*, **238**, 143 (2004).
(31) M. Suzuki, T. Yoshida, T. Koyama, S. Kobayashi, M. Kimura, K. Hanabusa, and H. Shirai, *Polymer*, **41**, 4531 (2000).
(32) Y. An, T. Koyama, K. Hanabusa, H. Shirai, J. Ikeda, H. Yoneno, and T. Itoh, *Polymer*, **36**, 2297 (1995).
(33) V. Gimenez, J. A. Reina, A. Mantecon, and V. Cadiz, *Polymer*, **40**, 2759 (1999).
(34) F. Chen and P. Liu, *AIChE J.*, **57**, 599 (2010).
(35) B. D. Chin and O. O. Park, *J. Colloid Interface Sci.*, **234**, 344 (2001).
(36) T. Hino, T. Namiki, and N. Kuramoto, *Synth. Met.*, **156**, 1327 (2006).
(37) S. Palaniappan and C. A. Amarnath, *React. Funct. Polym.*, **66**, 1741 (2006).
(38) R. K. Paul and C. K. S. Pillai, *Synth. Met.*, **114**, 27 (2000).
(39) T. M. Wu and Y. W. Lin, *Polymer*, **47**, 3576 (2006).
(40) H. Zhang, X. H. Wang, J. Li, Z. S. Mo, and F. Wang, *Polymer*, **50**, 2674 (2009).
(41) P. Ghosh, A. Chakrabarti, and S. K. Siddhanta, *Eur. Polym. J.*, **35**, 803 (1999).
(42) G. Rupali, D. Amitabha, and G. Goutan, *Synth. Met.*, **123**, 21 (2001).
(43) G. Rupali and D. Amitabha, *Synth. Met.*, **132**, 21 (2002).